Interactions of lipopolysaccharide with lipid membranes, raft models — A solid state NMR study

Filip Ciesielski [a], David C. Griffin [a], Michael Rittig [a], Ignacio Moriyón [b], Boyan B. Bonev [a,*]

[a] School of Biomedical Sciences, University of Nottingham, Nottingham NG7 2UH, UK
[b] Departamento de Microbiología, Universidad de Navarra, e Instituto de Salud Tropical, 31008 Pamplona, Spain

ARTICLE INFO

ABSTRACT

Lipopolysaccharide (LPS) is a major component of the external leaflet of bacterial outer membranes, key pro-inflammatory factor and an important mediator of host–pathogen interactions. In host cells it activates the complement along with a pro-inflammatory response *via* a TLR4-mediated signalling cascade and shows preference for cholesterol-containing membranes. Here, we use solid state ^{13}C and ^{31}P MAS NMR to investigate the interactions of LPS from three bacterial species, *Brucella melitensis*, *Klebsiella pneumoniae* and *Escherichia coli*, with mixed lipid membranes, raft models. All endotoxin types are found to be pyrophosphorylated and Klebsiellar LPS is phosphonylated, as well. Carbon-13 MAS NMR indicates an increase in lipid order in the presence of LPS. Longitudinal ^{31}P relaxation, providing a direct probe of LPS molecular and segmental mobility, reveals a significant reduction in ^{31}P T_1 times and lower molecular mobility in the presence of ternary lipid mixtures. Along with the ordering effect on membrane lipid, this suggests a preferential partitioning of LPS into ordered bilayer sphingomyelin/cholesterol-rich domains. We hypothesise that this is an important evolutionary drive for the selection of GPI-anchored raft-associated LPS-binding proteins as a first line of response to membrane-associated LPS.

© 2013 Elsevier B.V. All rights reserved.

1. Introduction

Lipopolysaccharide (LPS, or endotoxin) is the main component in the external leaflet of the Gram-negative bacterial outer membranes. Although LPS protects bacteria against some harmful molecules, it is readily recognised by host innate immunity receptors and defence systems. LPS is shed during cell division and bacterial death and plays an important part in Gram-negative pathogen/host recognition. The LPS of most Gram-negatives is a target of bactericidal peptides, activates the complement pathway and triggers a pro-inflammatory response, which may lead to complications accompanying acute infections, trauma and shock. In higher organisms, receptor-mediated signalling pathways act as an early detection system, which relies on recognition by LBP and CD14-MD-2-TLR4 to initiate NF-κB-mediated transcription of pro-inflammatory mediators, such as TNFα and IL1-β (reviewed in [1]). However, some bacteria have evolved LPS types that are poor activators of innate immunity, a trait that facilitates host invasion [2,3].

Most LPS molecules can be divided into three regions: a conserved hexa- or hepta-acyl disaccharide moiety, lipid A, which makes up the lipophilic domain and anchors LPS into the outer membrane; core oligosaccharide (subdivided into a highly conserved inner section and a variable outer core), and a long O-specific chain (Fig. 1). Often, the inner core of LPS and lipid A is phosphorylated and may be pyrophosphorylated [4]. Smooth-type LPS have all components present but mutations can generate rough LPS lacking the O-antigen and in some cases parts of the inner core.

Host cell membranes contain a complex proteolipid environment, which transmits cellular signals to the exterior and responds rapidly to changes in the cellular environment. It is now clear that the lipid constituent on the plasma membranes has the propensity to phase separate into small, cholesterol and sphingomyelin-rich domains (lipid rafts), which share a topologically continuous space with a more fluid, phosphatidylcholine-rich phase [5]. Lipid rafts preferentially sequester saturated-chain lipids and proteins with greater hydrophobic thickness while expelling unsaturated lipids and proteins with smaller hydrophobic thickness into the disordered phase. This heterogeneous environment permits lateral compartmentalization of membrane proteins [6] and changes in co-localization of proteins and complexes, as seen in LPS-mediated lymphocyte activation [7]. Lipid rafts often sequester GPI-anchored proteins [8], for example CD14 [9,10], and pro-inflammatory protein complexes [7]. Moreover, some pathogenic bacteria have evolved strategies for host colonization that specifically rely on targeting, recognition and engagement of lipid rafts [11–15].

In addition to TLR4-mediated activation, receptor-independent interactions that are essential to the survival of intestinal commensals
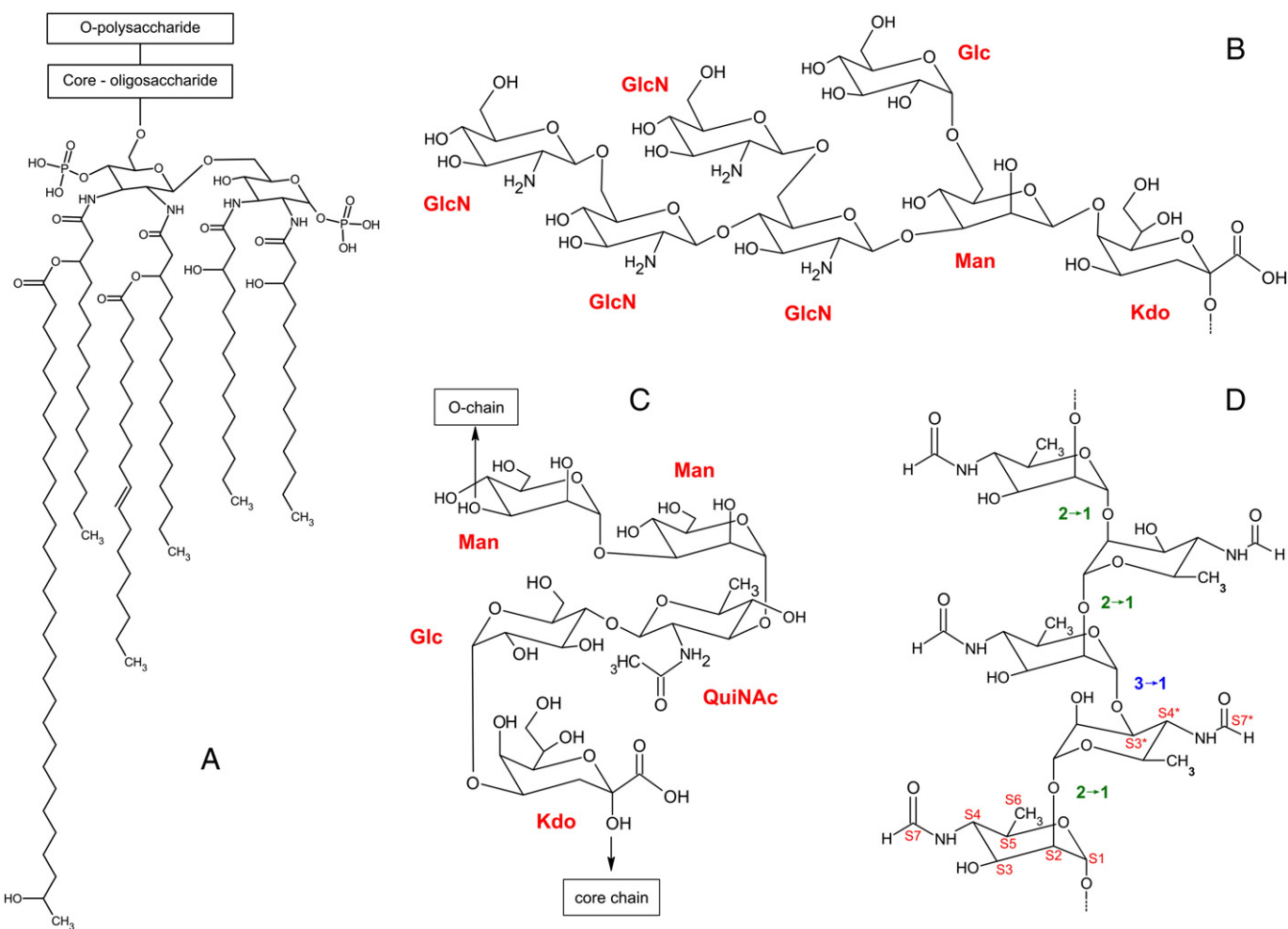
Fig. 1. Chemical structure of *B. melitensis* LPS: (A) lipid A (tentative structure based on *B. abortus* lipid A after [22,32]), core oligosaccharide (following [56]) (B), reducing end of O-polysaccharide (C) and the O-polysaccharide repeating unit (D).

within the host or are utilised in immunosilent host invasion, take place between bacterial LPS and host cell membranes [16]. Recently, we have shown that cholesterol in phase separated, raft-containing membranes plays an important role in LPS-membrane recognition, where LPS binds with higher affinity to phosphatidylcholine (PC), sphingomyelin (SM) and cholesterol-containing ternary lipid systems, raft models. Experiments in live cells show that LPS-binding to Jurkat T-lymphocyte membranes is reduced significantly after cholesterol removal [17]. Receptor-independent LPS binding to cholesterol-containing membranes is also dependent on LPS origin, with LPS from gut commensal *Escherichia coli* showing an order of magnitude weaker binding compared to LPS from the opportunistic pathogens *Salmonella enterica* and *Klebsiella pneumoniae* [17]. The presence of LPS in vesicles of *E. coli* lipid extracts has been shown to induce enlargement of gel-like areas and has been suggested to reflect the association of LPS with these areas [18].

In this study, we investigate the receptor-independent interactions between LPS from three bacterial species with model membranes and lipid membranes. Since quiescent TLR4 and LPS-recognition partners are not raft-associated, we hypothesise that preferential association of LPS with lipid rafts may give bacterial pathogens an advantage in avoiding immunodetection. In one example, LPS from *Brucella abortus* is known to internalize in macrophages as membrane vesicles and be presented subsequently to the cell surface as large membrane macrodomains [19]. These carry MHC-II but not MHC-I, thus impairing presentation of peptides to specific CD4+ T cell hybridomas [20]. We seek to assess the partitioning within laterally separated lipid

membranes of LPS from *Brucella melitensis*, a pathogen capable of invading host macrophages; from *K. pneumoniae*, a pathogen involved in respiratory infections, bacteraemia and septicaemia; and, from *E. coli*, a human gut commensal. The interaction between pathogen and host was modelled using LPS-containing dioleoyl phosphatidylcholine (PC_{100}) liposomes as LPS delivery vehicles, which present membrane endotoxin for binding to a host membrane model composed of PC, sphingomyelin (SM) and cholesterol in 55/15/30 molar ratio ($PC_{55}SM_{15}Cholesterol_{30}$). Lipid mixtures of this composition are known to undergo phase decomposition under ambient conditions into ordered SM/cholesterol-rich domains surrounded by fluid PC-rich phase [21]. We used high resolution solid state magic angle spinning (MAS) NMR to study the incorporation of LPS into membranes composed of $PC_{55}SM_{15}Cholesterol_{30}$ using LPS binding to pure PC_{100} membranes as a control. Changes in molecular mobility of membrane lipid constituents after the addition of LPS were followed by high-resolution ^{13}C CP MAS NMR. Preferential segregation of LPS from *E. coli*, *K. pneumoniae* and *B. melitensis* into specific lateral membrane environments was investigated by ^{31}P MAS solid state NMR. Phosphate, pyrophosphate and phosphonate ^{31}P resonances were used as internal reporters of changes in LPS, PC100 and SM molecular mobility, which are followed by ^{31}P longitudinal relaxation.

2. Materials and methods

All lipids were purchased at >98% purity and used without further purification. Cholesterol was obtained from Sigma (Pace, UK) while DOPC

(1,2-dioleoyl-sn-glycero-3-phosphatidylcholine) and sphingomyelin were obtained from Avanti Polar Lipids (Alabaster, Alabama, U.S.A.). Lipopolysaccharide from *E. coli*, O111, *S. enterica typhimurium* and *K. pneumoniae* was purchased from Sigma (UK) at 40–60% purity and was subsequently purified [22]. LPS from *B. melitensis* 16 M was prepared in house and purified as detailed below following Velasco et al. [22].

2.1. LPS purification

Commercial LPS, containing approximately 50% nucleic acids, was suspended in buffer (10 mM Tris, pH 7.4) at a concentration of 10 mg/ml and treated with DNase and RNase (50 μg of DNase and 50 μg of RNase per 10 mg of crude LPS) at 37 °C for 30 min. This was followed by incubation at 55 °C in proteinase K (50 μg per 10 mg of LPS) for 3 h and room temperature with a fresh batch of proteinase K for 8–16 h. The cycle was repeated and LPS was precipitated with 4 volumes of cold methanol at −18 °C for 2 h. The precipitate was recovered by centrifugation (6000 x*g*, 15 min, 4 °C) and residual methanol was removed under vacuum or dialyzed and freeze-dried. In addition, for *B. melitensis* LPS, the dry product was resuspended in deionized distilled water and extracted three times with an equal volume of chloroform:methanol (2:1) to remove LPS-associated phospholipids and amino lipids.

2.2. Membrane preparation

Single lipid membranes of DPPC or DOPC were prepared by suspending the lipid in deionised water and mixing the suspension vigorously for 15 min at 45 °C using a fine glass rod. The lipid suspensions were freeze-thawed between liquid nitrogen and 50 °C water bath for a minimum of 5 cycles. Multilamellar vesicles (MLV) were centrifuged at 16,000 x*g* for 10 min (Biofuge pico, Heraeus) and the pellets loaded in 4.0 MAS NMR rotors. Sample hydration was estimated at 2.7-fold by weight or approximately 100 water molecules per lipid.

Mixed lipid membranes of DOPC/cholesterol (2:1 molar ratio) or DOPC/SM/cholesterol (55:15:30 molar ratio), $DOPC_{55}SM_{15}Chol_{30}$, were prepared by co-dissolving in 2:1 methanol/CHCl$_3$, removing the solvent under high vacuum and hydrating the film. Pure water was used instead of buffering solutions to reduce sample heating during NMR measurements. In the presence of LPS, lipid suspensions were difficult to pellet due to the electrostatic repulsion and hydrated samples were first freeze-dried, loaded in the NMR rotors, and then resuspended in 50 μl of deionised water. Reference membrane samples without LPS were treated in the same way.

2.3. LPS-containing membranes

LPS was suspended in distilled water and incubated at 56 °C for 15 min, vortexed for 2 min and cooled to 4 °C, then the cycle was repeated two more times. LPS suspensions were stored at 4 °C for up to 4 h before incubation with lipid membranes. Lipid bilayers were prepared as single unilamellar vesicle (SUV) suspensions to maximise membrane availability and to facilitate LPS insertion. Dry lipid films were hydrated with de-ionised water (0.5 ml per 10–20 mg of lipid) and hydrated suspensions were sonicated for 30 min. LPS suspensions were then heated to 50 °C and incubated with SUV suspensions for 10 min. Samples were then freeze-dried, loaded in the MAS NMR rotors and resuspended in 50 μl of de-ionised water.

2.4. Mixing DOPC/LPS with DOPC/SM/Chol vesicles

To model pathogen/host membrane interactions, DOPC/LPS and $DOPC_{55}SM_{15}Chol_{30}$ vesicles were prepared separately, mixed, incubated at room temperature for 1 h and freeze dried. The dry pellets were loaded into 4 mm NMR rotors and hydrated with de-ionised water.

2.5. Solid state NMR spectroscopy

Solid-state NMR experiments were carried out on a Varian 400 MHz VNMRS direct drive spectrometer equipped with a 4 mm T3 MAS NMR probe (Varian, Palo Alto CA, USA) and temperature was regulated using balanced heated/vortex tube-cooled gas flow [23,24]. All ^{13}C spectra were referenced externally to adamantine CH$_2$ at 37.54 ppm, while ^{31}P spectra were referenced externally to 10% H$_3$PO$_4$ at 0 ppm.

High resolution cross-polarization [25] magic angle spinning, CP-MAS, spectra were acquired after 104 kHz proton excitation and 3.5 ms of 45 kHz Hartmann–Hahn contact using a proton ramp [26]. Heteronuclear proton couplings were removed under 66 or 45 kHz SPINAL-64 decoupling [27] in ^{13}C or ^{31}P spectra, respectively. Spectral acquisitions were repeated at 5 s interpulse delay, which exceeds approximately five-fold the ^{1}H longitudinal relaxation time for protons in lipids, and 1024 transients were averaged in acquisition. Inversion recovery was used to investigate ^{31}P longitudinal relaxation with delay times ranging from 1 ms to 5 s for phosphates and from 1 ms to 1 s for pyrophosphate and phosphonate resonances. The interpulse delay in these experiments was set to 20 s. Relaxation times were obtained assuming a single dominant relaxation mechanism.

Spectra were processed and analysed using ACD/Labs (Advanced Chemistry Development, Inc., Toronto, Canada). Homogeneous broadening was assumed and resonances were approximated by fitting Gauss-Lorentzian lineshapes. In cases of closely spaced resonances showing significant overlap, spectral deconvolution was carried out using Felix (Accelrys Inc., San Diego, CA, USA) and ACD/Labs.

3. Results

The role membrane heterogeneities play in LPS-mediated pathogen/host interactions was investigated after LPS-containing PC liposomes, bacterial outer membrane models, were incubated with $PC_{55}SM_{15}Cholesterol_{30}$ vesicles mimicking host membranes. The $PC_{55}SM_{15}Cholesterol_{30}$ triple mixtures separate into ordered domains, SM/cholesterol-rich lipid rafts, and a fluid, PC-rich phase [21]. Changes in membrane lipid dynamics after LPS incorporation into $PC_{55}SM_{15}Cholesterol_{30}$ membranes *vs.* PC_{100} membranes were followed by high resolution ^{13}C MAS NMR. Differences in LPS molecular mobility between $PC_{55}SM_{15}Cholesterol_{30}$ and in PC_{100} membranes were compared using ^{31}P MAS longitudinal relaxation. Reduction in LPS ^{31}P mobility was taken as an indication of LPS partitioning into ordered domains (raft models).

3.1. Carbon-13 MAS solid state NMR

The interactions between LPS and DOPC (PC_{100}) membranes were investigated by high-resolution ^{13}C MAS solid state NMR for comparison with LPS–raft interactions within ternary lipid mixtures. LPS from *B. melitensis*, *K. pneumonia* and *E. coli* was incorporated into PC_{100} membranes. A single pulse excitation ^{13}C MAS NMR spectrum from *B. melitensis* LPS in PC_{100} membranes, 1:1 w/w, is shown in Fig. 2A. DOPC resonances were assigned as previously described [28,29]. Where resolved, LPS ^{13}C resonances were assigned using spectroscopy with spectral prediction (ACD Labs) and according to [30]. Because LPS structure contains a large number of pyranose units, observed resonances are group-assigned to formylperosamine (Rha4N) O-chain polysaccharide and lipid A (Fig. 1D), as segmental mobility with this region is sufficiently fast in comparison to the NMR timescale to allow efficient decoupling and signal acquisition [24]. Methyl resonances at 16.7 and 17.0 ppm (Fig. 2B) can be attributed to O pyranose-3 methylation sites (Fig. 1D). Resonances at 51.0
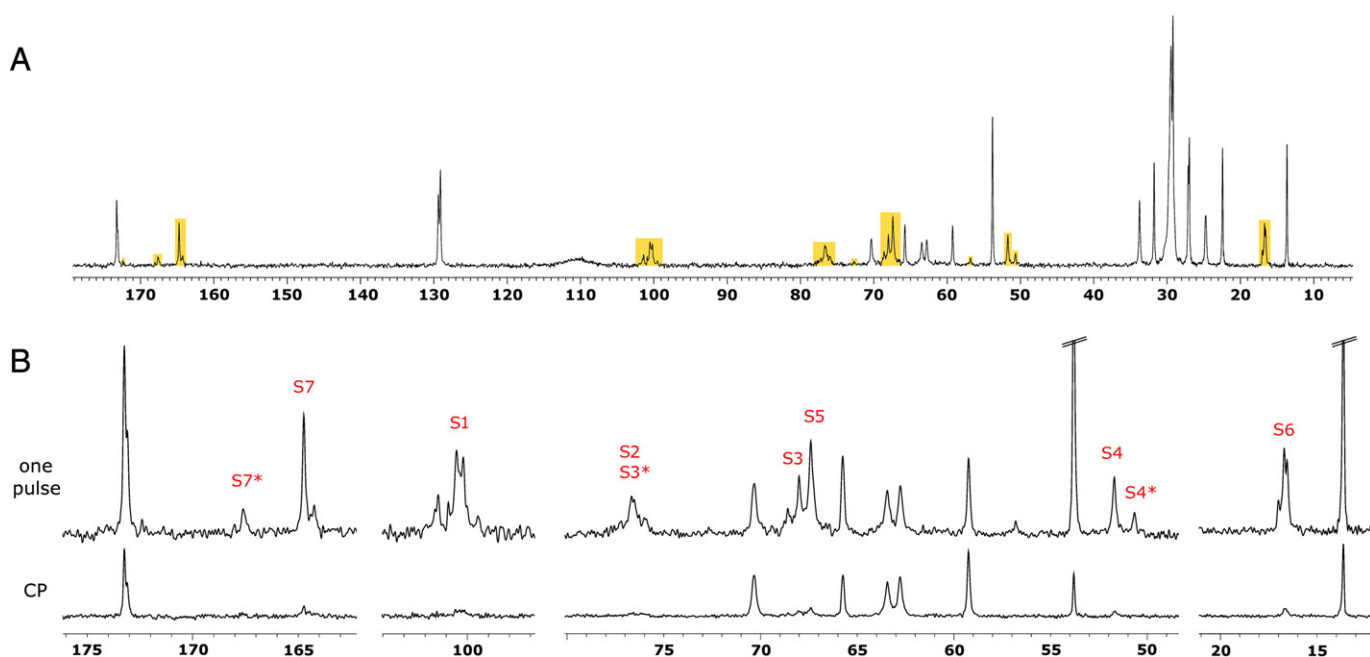
Fig. 2. Carbon-13 MAS NMR spectra of DOPC/LPS from *B. melitensis*. (A) One pulse excitation with SPINAL decoupling; LPS peaks are highlighted yellow and assigned in B,C; (B) and (C) show comparison between one pulse experiment (top line) and CP (bottom); (D) chemical structure of the O-polysaccharide sugar unit from *B. melitensis* LPS; the unit is a polymeric chain of 5 N-formylperosamine monosugars, four of which are connected *via* glycosidic bond between carbons nos. 2 and 1 (green labels) and one of which is connected in a 3 → 1 fashion (blue label).

and 52.0 ppm can be assigned to O-chain Rha4N carbons. The resonance at 57.0 ppm (Fig. 2B) can be assigned to outer core GlcN-2 aminated carbon. Spectral intensity between 65 and 70 ppm is likely to arise from Rha4N 3 and 5 carbons in the O-chain and GlcN 3 and 5 carbons in the core, while intensity between 77 and 80 ppm can be attributed to O-chain carbons in positions 4,2 involved in glycosidic bonds. Resonances within these groups are difficult to assign conclusively from 1D spectra alone. The group of resonances between 100.0 and 102.0 ppm arises mostly from Rha4N-1 and Kdo-1 carbons and the signal near 100 ppm can be attributed to less mobile Kdo from the core region nearer lipid A that links the core to the lipid A saccharide backbone. Resonances arising from O-chain formylperosamine carbon 7 are resolved at near 165 and 168 ppm. Lipid A and inner core acetyl resonances appear close to and partially overlap the DOPC carbonyls at 173 ppm, as observed by others in ^{13}C-labelled LPS [31]. Comparison to CP spectra, Fig. 2B, reveals a significant diminution in LPS resonance intensity due to interference of molecular motions on the intermediate timescale with ^{1}H–^{13}C magnetization transfer. Richer spectral features are revealed at higher temperatures where LPS chains enter the L_α phase and cooperative axial molecular rotation becomes dominant within the bilayer. However, under such conditions we observed gradual degradation of LPS.

Carbon-13 MAS NMR was also used to investigate LPS from *K. pneumoniae* in DOPC bilayers. In contrast to brucellar LPS, resonances arising from klebsiellar LPS had significantly lower intensity both in single pulse excitation and in CP MAS spectra. Similar situation was reported by Nomura et al. [31], who observed low intensity resonances even from ^{13}C-labelled rough-type LPS. This observation is likely to reflect a significantly higher mobility within the klebsiellar than within the brucellar LPS. This is reasonable as the latter has been known to have very long acyl chains which can possibly span membrane bilayers and affect LPS mobility [32]. Smooth-type LPS from *E. coli*, embedded in DOPC, produced no discernible resonances with either direct ^{13}C excitation or CP. In addition to segmental mobility and cooperative molecular rotation, greater angular excursions of the LPS molecules within the bilayer are likely to interfere with the NMR measurements. The interaction between *E. coli* LPS and membranes is comparatively weaker, seen in a 20-fold higher dissociation constant for *E. coli* LPS in binding to lipid membranes by comparison to LPS from *K. pneumoniae* [17], and leads to further NMR signal diminution.

To simulate host/pathogen interactions, liposomes of DOPC and LPS from *B. melitensis* were mixed with $PC_{55}SM_{15}Cholesterol_{30}$ vesicles and the effects of LPS on the membrane lipid were investigated by ^{13}C CP-MAS NMR. Spectra from LPS/PC_{100} are shown in Fig. 3, bottom, alongside spectra from $LPS/PC_{55}SM_{15}Cholesterol_{30}$, top. Besides diminution in LPS intensity resulting from the addition of membrane lipid, the effect of mixing the two lipid systems appears to be non-uniform across the spectrum, leaving measurable intensity only from more mobile S6 methyl carbons (Fig. 2). Resonances from LPS ring carbons S3, S5 and S7, resolved in PC_{100} membranes, leave no discernible intensity after fusion with $PC_{55}SM_{15}Cholesterol_{30}$ membranes. Such selective restriction in segmental mobility can be associated with specific molecular interactions, as previously shown for binding of PrP to ganglioside GM1 in lipid rafts [33] and is consistent with partitioning of *B. melitensis* LPS into the motionally restricted lateral environment of the cholesterol/SM-rich membrane sub-phase.

The ordered, raft-like sub-phase of $PC_{55}SM_{15}Cholesterol_{30}$ membranes, is enriched in SM and cholesterol while PC is preferentially expelled into a more mobile lateral environment. We used solid state ^{13}C CP MAS NMR to compare the effect of LPS incorporation on the SM/cholesterol-rich phase by comparison to the PC-rich phase. CP MAS NMR spectrum from $PC_{55}SM_{15}Cholesterol_{30}$ membranes is shown in Fig. 4A–C, upper traces, with characteristic spectral regions enlarged in Fig. 4D–G and assigned according to [28,34,35]. The ternary lipid vesicles were then co-incubated with *B. melitensis* LPS/PC_{100} liposomes and the resulting spectra are shown in Fig. 4, lower traces. An overall reduction in spectral intensity of SM and cholesterol resonances, which results from dilution with additional DOPC, was accompanied by non-uniform intensity diminution across the spectrum and increase in linewidth for some resonances. By contrast, DOPC resonances remained largely unaffected after the addition of LPS and were used as an internal standard. These observations are consistent with co-incorporation of LPS into the SM/cholesterol-rich bilayer phase.
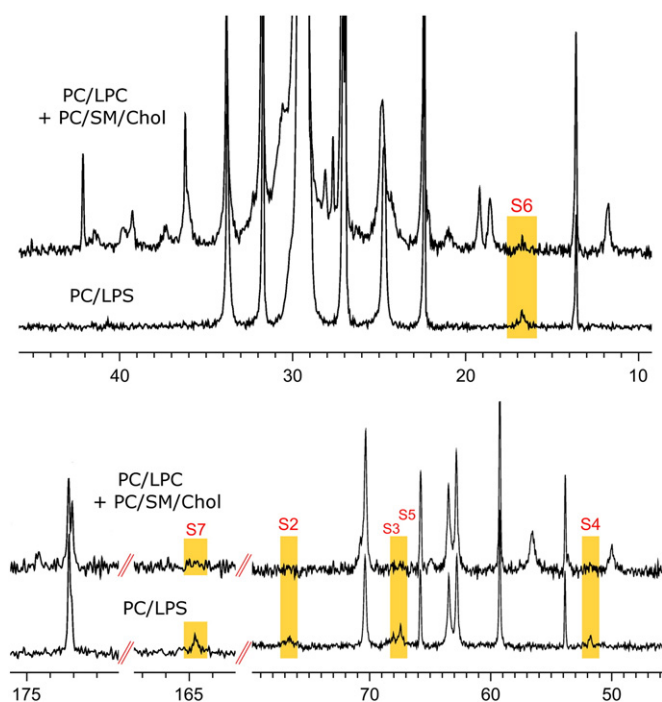
Fig. 3. Natural abundance ^{13}C CP-MAS NMR spectra from *B. melitensis* LPS in DOPC membrane; (A) comparison of DOPC/LPS spectra before (bottom plot) and after (top plot) addition of DOPC/SM/Cholesterol vesicles; (B,C) Selected LPS peaks (S4 and S5) from ^{13}C CP-MAS NMR experiment with *B. melitensis* LPS in DOPC bilayer acquired at 3.5 ms contact time before (bottom) and after (middle) addition of DOPC/SM/cholesterol; the latter sample (with PC/SM/Chol) was then repeated using 1.5 ms contact time (top).

The addition of brucellar LPS to $PC_{55}SM_{15}Cholesterol_{30}$ vesicles resulted in slight shift in some DOPC resonances, leaving intensity and linewidth unaffected. By contrast, noticeable broadening and a decrease in peak intensity were observed for SM and cholesterol resonances (Fig. 4), which is consistent with a selective incorporation of LPS into the SM and cholesterol-rich sub-phase. The melting temperature of *B. melitensis* LPS acyl chains is on the order of 35–40 °C [36], which suggests that LPS addition leads to an increase in the chain order and reduction in molecular mobility within the raft phase, specifically of SM and cholesterol. The effects of LPS from *K. pneumonia* and *E. coli* on $PC_{55}SM_{15}Cholesterol_{30}$ membranes were very similar (Fig. 5).

3.2. Phosphorous-31 MAS NMR

Phosphorus-31 MAS NMR was used to investigate membrane lipid phosphates and to follow molecular dynamics within $PC_{55}SM_{15}Cholesterol_{30}$ membranes. Phosphate groups in DOPC and SM give rise to strong resonances at -0.9 and 0.3 ppm, respectively [37,38], seen in the spectrum of Fig. 6. Longitudinal relaxation times were obtained from PC and SM phosphates by inversion recovery at 15 and 25 °C to assess phospholipid molecular mobility rates. T_1 values were very similar from PC and SM, which suggests proximity to T_1 minimum for both lipids and that molecular dynamics within the ternary mixture is dominated by motions with correlation times on the order of 10 ns.

Phosphorus-31 MAS NMR spectra from $PC_{55}SM_{15}Cholesterol_{30}$ membranes, incubated with DOPC vesicles containing LPS from *B. melitensis*, *K. pneumoniae* and *E. coli*, are shown in Fig. 7. Spectral intensity is dominated by the PC phosphates at -0.9 ppm and LPS phosphates at 1.0 ppm, respectively, and spectra have been truncated vertically to show LPS phosporylation. *K. pneumoniae* and *E. coli* LPS core oligosaccharide and lipid A sugars are phosphorylated,

which can be seen as a resonance at 3.2 and 1.6 ppm, respectively [39] (Fig. 7B,C). Phosphorylation of *B. melitensis* LPS, significantly overlaps with the PC resonance and cannot be resolved from the MAS spectrum without selective spectral excitation (Fig. 7A). All three types of LPS are pyrophosphorylated, which gives rise to overlapping intensity at -11.6 ppm for *B. melitensis* LPS (Fig. 7A) or well-resolved resonances at -8.0 and -12.5 ppm for *K. pneumoniae* LPS and -6.4 and -11.6 ppm for *E. coli* LPS (Fig. 7B,C respectively) [40]. A well-resolved resonance at 19.9 ppm in Fig. 7B suggests that *K. pneumoniae* LPS is also phosphonylated [41]. Residual intensity near 19 ppm in the spectrum of Fig. 7C suggests that *E. coli* LPS may undergo phosphonylation, as well as seen in capsular polysaccharides [42]. Phosphonylation can be observed following periods of phosphorus starvation during bacterial growth.

3.3. Phosphorus-31 longitudinal relaxation

Phosphorus-31 longitudinal relaxation times, T_1, offer an intrinsic measure of changes in molecular mobility of membrane LPS and phospholipids. Longitudinal relaxation was measured from SM and DOPC resonances within $PC_{55}SM_{15}Cholesterol_{30}$ membranes at 25 °C and 15 °C to assess the rates of fast molecular motions ($\sim$ns) by comparison to the nuclear precession frequency (Fig. 6). Values of T_1 were on the order of 0.9 s for both lipids and were not affected significantly by temperature with PC relaxation times possibly decreasing slightly at 25 °C. This suggests mobility near T_1 minimum and that fast lipid mobility within both lipid species occurs on the order of 6 to 10 ns timescale or fast/slow motional regimes of phospholipids residing in the fluid phase and in the ordered domains, respectively. By comparison, molecular mobility within fluid DOPC membranes is fast in comparison to the NMR timescale [43]. Over the temperature range, explored in this study, $PC_{55}SM_{15}Cholesterol_{30}$ membranes undergo lateral phase decomposition into ordered lateral domains and fluid, PC-rich, phase [21]. The observed relaxation times are the average from the two environments.

Using inversion recovery MAS NMR, ^{31}P T_1 values were obtained from LPS pyrophosphates (PP) and phosphonates (Pna), as well as mean values from phosphates (P) including contributions from PC, SM and LPS. Phosphorus-31 relaxation times from LPS from *B. melitensis* (A), *K. pneumoniae* (B) and *E. coli* (C) in PC bilayers, as well as LPS in $PC_{55}SM_{15}Cholesterol_{30}$ membranes, are shown in Fig. 8 and summarised in Table 1. Pyrophosphate relaxation times from *B. melitensis* LPS (Fig. 8A) were comparatively short, on the order of 100 ms and increased with temperature within both types of membranes, which indicates that molecular mobility occurs in the fast regime. The observed T_1 values were reduced from 100 ms in DOPC to approximately 25–40 ms in the $PC_{55}SM_{15}Cholesterol_{30}$ membranes, which indicates a reduction in LPS pyrophosphate mobility. Such reduction in mobility is consistent with preferential partitioning of brucellar LPS within the motionally restricted SM/cholesterol-rich raft domains. Phosphate T_1 values measured within each type of LPS-containing membranes were on the order of 0.5 s and slightly decreased with temperature, which suggests the dominant molecular motions, giving rise to longitudinal relaxation, occur in the slow regime but mean relaxation times remain near T_1 minimum. This is consistent with the observed shorter T_1 within the more mobile DOPC/LPS bilayers by comparison to the motionally restricted $PC_{55}SM_{15}Cholesterol_{30}$ membranes. While stating this, we must remain mindful of the average nature of the observed monophosphate T_1 values.

Phosphorus-31 relaxation times of *K. pneumoniae* LPS pyrophosphates, examined at 15 and 25 °C were significantly longer than in *B. melitensis*, nearing 0.5 s in PC_{100} and over 1 s in $PC_{55}SM_{15}Cholesterol_{30}$ membranes. Values of T_1 increase with temperature for both -9 ppm and -13 ppm resonances, suggesting both PP phosphates are undergoing fast motions,
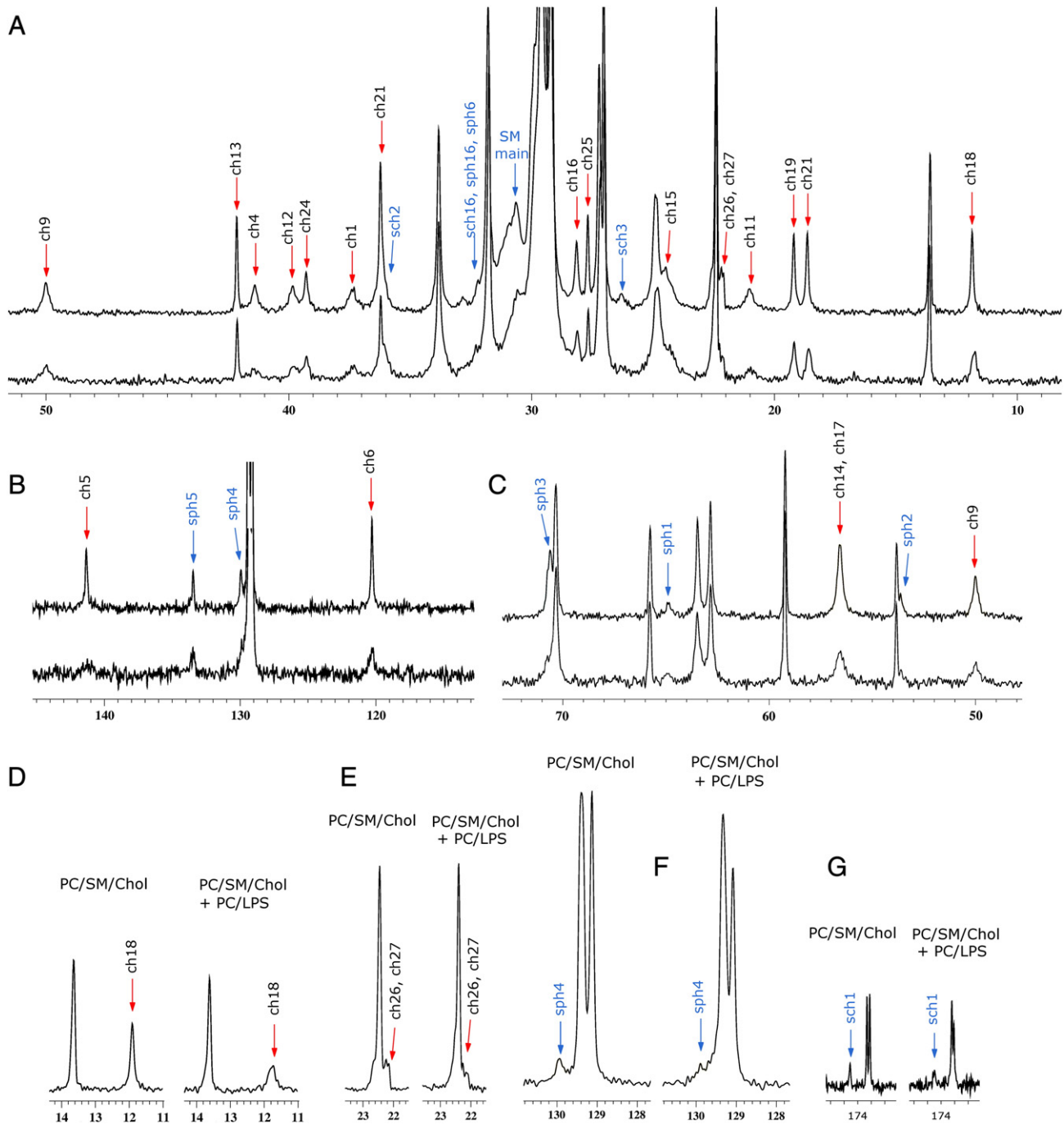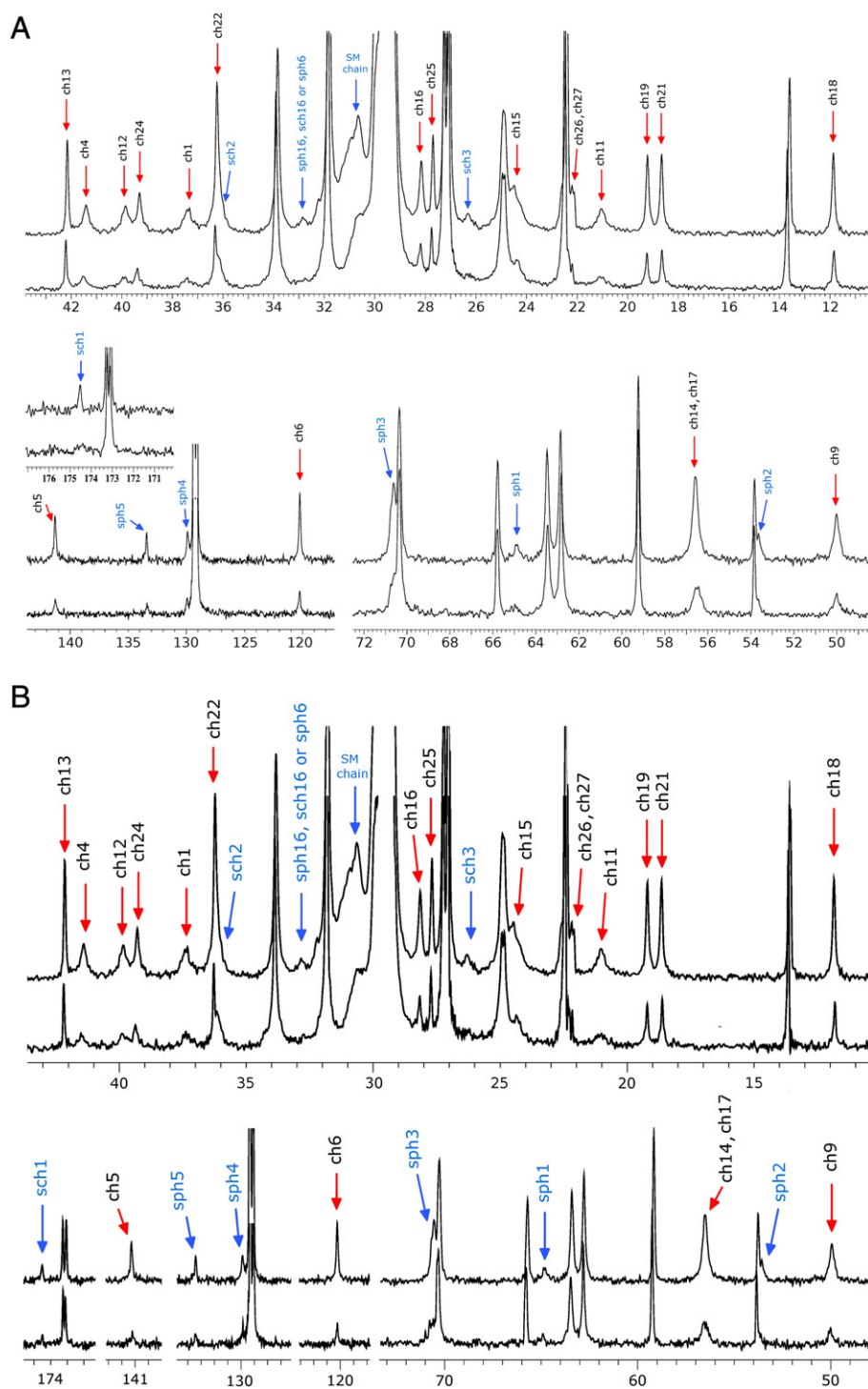
Fig. 4. Natural abundance ^{13}C CP-MAS NMR spectra of DOPC/SM/cholesterol vesicles (top spectra) and of DOPC/LPS from *B. melitensis* mixed with DOPC/SM/cholesterol vesicles (bottom spectra). (A) the main hydrophobic chain region; (B) the double bond region; (C) the head-group region; (D–G) selected peaks from the spectrum showing changes to SM or Chol peaks: (D) the DOPC methyl group L18 and cholesterol ch18; (E) carbon L17 peak and cholesterol ch26 and ch27; (F) DOPC double bond L9/10 and sphingomyelin sph 5; (G) DOPC carbonyl L1 and sphingomyelin sph1.

although values were relatively close and fell within the variance range (Fig. 8B). Pyrophosphate T_1 values from LPS markedly increased between PC and $PC_{55}SM_{15}Cholesterol_{30}$ membranes. This is puzzling, as highest molecular mobility within the mixed lipid membranes would be expected in the PC-rich sub-phase where T_1 values should be similar to or shorter than those in pure PC membranes. This can be rationalised if one considers the pyrophosphate location within lipid A, where mobility is tightly coupled to that of the membrane lipid. In this case, the principal contribution to ^{31}P relaxation comes from molecular librations, either independent on the local scale or collective, as part of the membrane thermal undulations. In the presence of cholesterol within

$PC_{55}SM_{15}Cholesterol_{30}$ membranes, molecular vibrations are restricted, while axial molecular mobility is unaffected with the latter becoming the dominant relaxation mechanism. This interpretation brings into agreement the observed relaxation trends in the PP with those of the Pna (see below), both suggesting restrictions in LPS mobility and segregation into cholesterol-rich lateral domains. This is unsurprising, as the LPS lipid chains are usually saturated with a main chain melting transition temperature around 35–40 °C [44].

Relaxation times of the phosphonate resonance, observed at 20 ppm in klebsiellar LPS, increase with temperature in the ternary mixture, which is indicative of fast molecular mobility. In contrast

Fig. 5. Natural abundance ^{13}C CP-MAS NMR spectra of DOPC/SM/cholesterol vesicles (upper lines) and of DOPC/LPS mixed with DOPC/SM/Chol vesicles at 30 °C (bottom lines). (A) DOPC/LPS with the endotoxin from *K. pneumonia* and (B) from *E. coli*.

to pyrophosphates, a marked reduction in phosphonate T_1 values was observed between DOPC and $PC_{55}SM_{15}Cholesterol_{30}$ membranes (Fig. 8B). This is consistent with a reduction in motional freedom of the phosphonates and with increased motional restrictions on the LPS molecules in the $PC_{55}SM_{15}Cholesterol_{30}$ membranes. Segmental flexibility within the core oligosaccharide uncouples the Pna from molecular librations within the lipid A region and relaxation is likely dominated by fast molecular rotation, as seen from the significantly higher T_1 values for Pna than PP in PC membranes.

Pyrophosphate ^{31}P relaxation times from *E. coli* LPS were on the order of 850–900 ms in DOPC bilayers and were reduced to approximately 300 ms in $PC_{55}SM_{15}Cholesterol_{30}$ membranes. Decrease in T_1 between 15 °C and 25 °C for both the −7 ppm and −11 ppm pyrophosphate resonances of LPS suggests that within $PC_{55}SM_{15}Cholesterol_{30}$ membranes molecular mobility occurs in the slow regime. Comparison of LPS pyrophosphate relaxation in PC membranes at 25 and 15 °C shows reduction in T_1 values from approximately 800 ms to near 350 ms, which points to fast motions as the dominant contribution
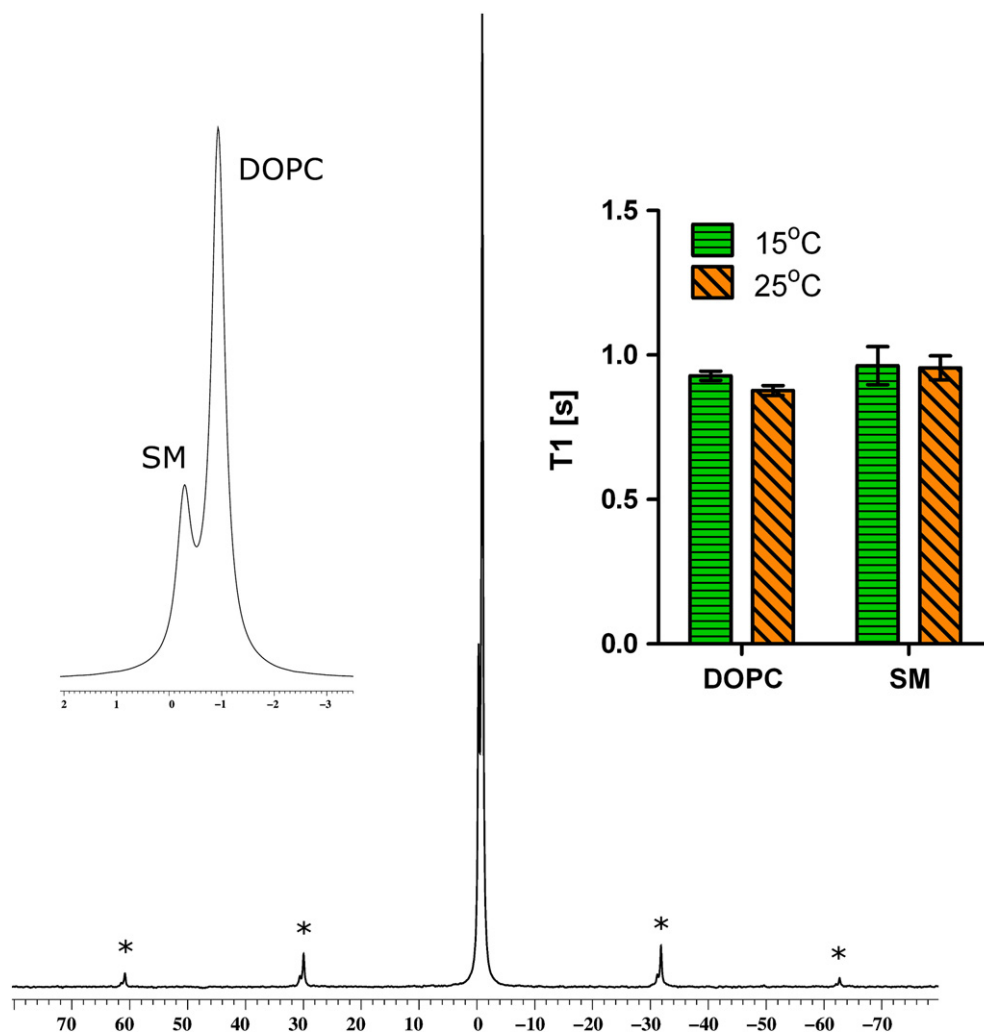
Fig. 6. Single pulse excitation ^{31}P MAS NMR spectrum of DOPC/SM/cholesterol (in 55–15–30 molar ratio respectively) taken at 25 °C. Spinning side-bands are indicated with * and the inlet in the left corner shows the main peak area around 0 ppm. The histograms show T_1 relaxation time constants measured for SM and DOPC.

to ^{31}P relaxation. Together with the dominance of slow motions in the PP relaxation in $PC_{55}SM_{15}Cholesterol_{30}$ membranes, this suggests preferential partitioning of LPS into the ordered lateral bilayer environment.

4. Discussion

Bacterial co-evolution with the host has delivered a sophisticated pathogen detection system, aimed at bacterial isolation and removal, paralleled by bacterial adaptations permitting immunosilent host invasion, as well as symbiotic co-existence between gut commensals and the host. LPS carries molecular signatures that create a pathogen-associated molecular pattern used by host defences for bacterial detection and subsequent clearing. In many cases pathogenic bacteria can provoke inflammatory responses that, although important for an effective activation of adaptive immunity, may compromise protective host layers and facilitate infection of otherwise non-compromised loci [45]. One way pathogenic bacteria have developed to modulate host defences is through membrane microdomains enriched in cholesterol and sphingomyelin [15,46]. Such domains appear to play an important role in the host cell by allowing lateral compartmentalization of cell surface proteins and re-compartmentalization in some cases of cell surface receptor activation [47–51] and of GPI-anchored proteins [9,52].

While receptor-mediated interactions between bacteria or their outer membrane LPS and host cells is an important mechanism for pathogen recognition, internalization and survival, it has become clear that bacterial LPS has selective preference for binding to cholesterol-containing membranes [17]. This effect depends on the bacterial origin of LPS and is stronger in true pathogens by comparison to gut commensal bacteria (*ibid.*). When binding to laterally phase-separated membranes, raft models, LPS causes amalgamation of cholesterol-containing domains into larges sub-phases with reduced line boundary, within which molecular mobility is lower [31].

We have explored the interactions between bacteria and cells through a model of bacterial outer membranes, in which LPS is delivered as a component of PC vesicles to ternary lipid mixture liposomes of $PC_{55}SM_{15}Cholesterol_{30}$, host membrane mimics. Carbon-13 MAS NMR was used to assess the effect of LPS presence on lipid dynamics and revealed preferential reduction in the overall molecular mobility within the combined fused vesicles in agreement with previous observations [31]. It is reasonable to expect such effect as the LPS chains are mostly saturated and likely to partition with preference into the ordered bilayer phase.

Phosphorus-31 relaxation suggests that LPS from all bacteria tested appears to have a weak ordering effect on the membrane lipid, although the low molar availability of endotoxin makes a more definitive assessment difficult. This observation supports the overall picture emerging from the ^{13}C measurements and ^1H relaxation, reported
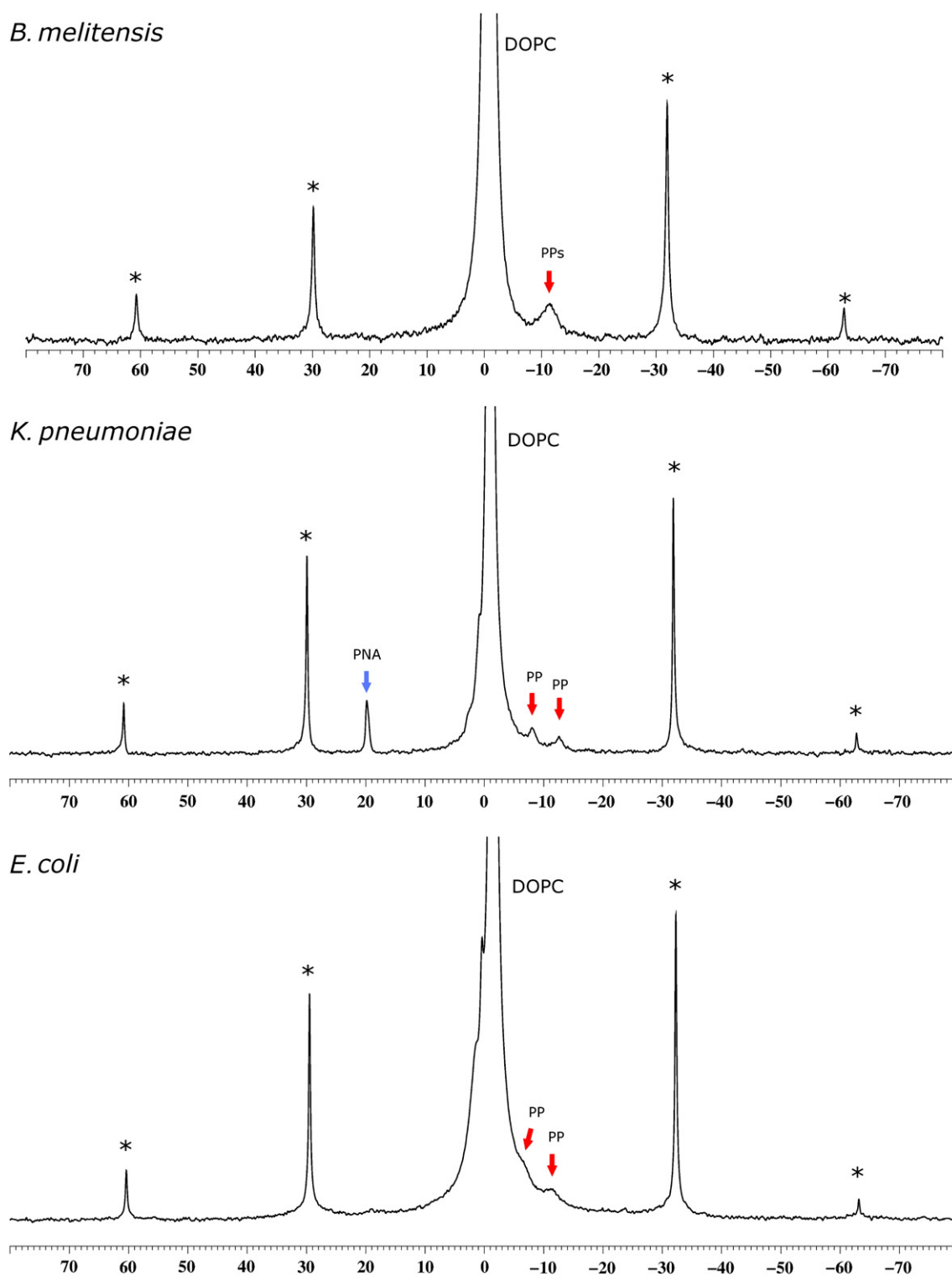
Fig. 7. Phosphorus-31 MAS NMR spectra of DOPC/LPS samples with endotoxin from three different bacterial strains: *B. melitensis* (top), *K. pneumoniae* (middle) and *E. coli* (bottom). The main peak at −1 ppm originates from the phosphate group in DOPC and it has two sidebands on both sides (labelled with *).

previously [31], of an overall membrane ordering effect LPS has on the ternary lipid mixtures.

Bacterial LPS is often phosphorylated in the lipid A moiety [53] and in some cases pyrophosphorylated either on a heptose residue in core oligosaccharide region or in lipid A [4]. Lipid A phosphates, derivatised to ethanolamine pyrophosphates, have been reported to occur with higher frequency in polymyxin-resistant *Salmonella* [54].

In this study, high resolution ^{31}P MAS NMR revealed that LPS from all three species investigated, *B. melitensis*, *K. pneumoniae* and *E. coli*, was pyrophosphorylated. Thus far, the presence of pyrophosphate has not been reported for *Brucella* LPS. However, genetic and mass spectral analyses show that *B. melitensis* lipid A contains ethanolamine, which could be present as the corresponding pyrophosphate (Gil-Ramírez, Y., Moriyón, I. and M. Iriarte, unpublished results).

A

B

C
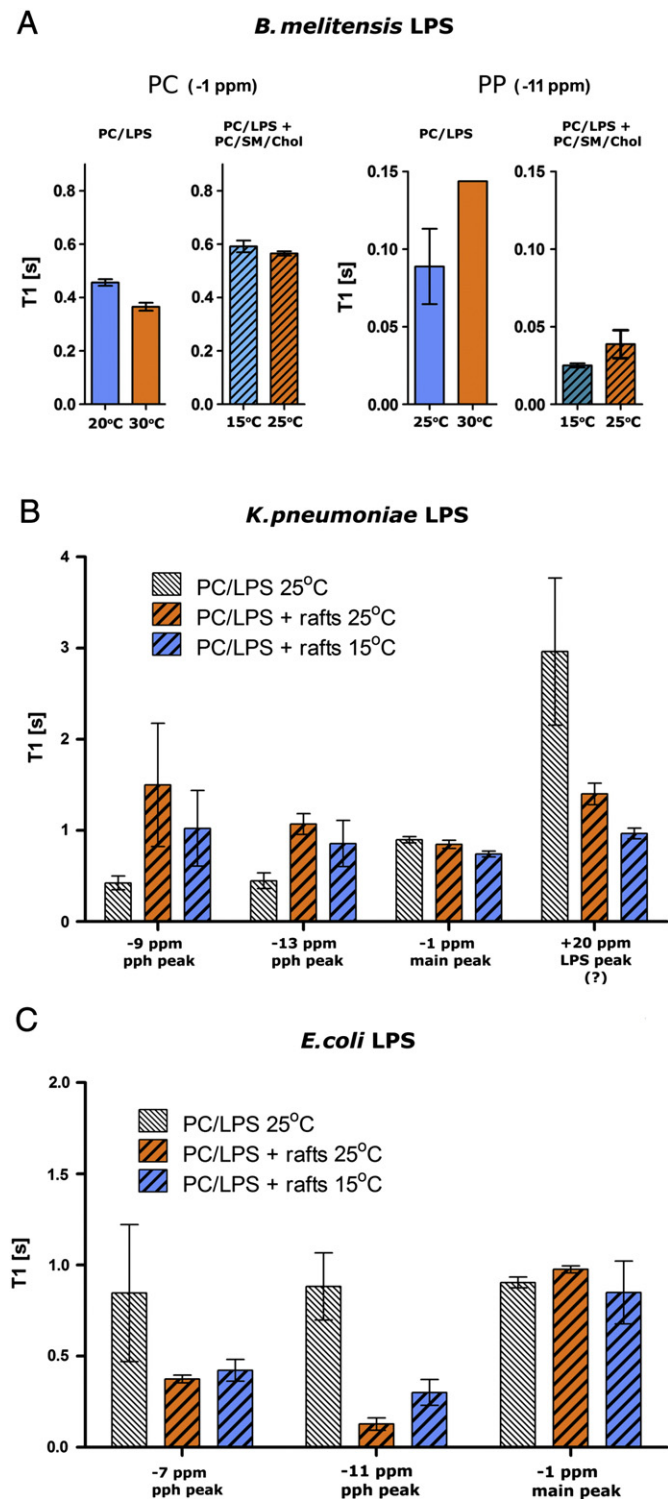
Fig. 8. Longitudinal relaxation T_1 time constants measured for DOPC/LPS before and after the addition of DOPC/SM/cholesterol vesicles. T_1 values determined for DOPC principal peaks and for LPS pyrophosphates; LPS from three bacterial species was studied: *B. melitensis* (A), *K. pneumoniae* (B) and *E. coli* (C).

Somewhat unusual, phosphonylation was observed in *K. pneumoniae* LPS, which is atypical of LPS but is observed in capsid polysaccharides, for example in *Neisseriaceae* [42]. Spectroscopic traces of, possibly transient, phosphonylation were observed in *E. coli* LPS, as well. Bacterial phosphonylation pathways are usually activated in phosphorus-poor growth conditions and the observed LPS phosphonylation may reflect phosphorus-starvation prior to LPS harvesting.

Table 1
T_1 relaxation times from ^{13}P NMR experiments carried out at 25 °C with DOPC/LPS before and after the addition of DOPC/SM/cholesterol vesicles.

B. melitensis:					
Resonance	T_1 in DOPC [s]			T_1 in PC/SM/Chol [s]	
	20 °C	25 °C	30 °C	25 °C	15 °C
−1 ppm (P)	0.46	–	0.37	0.57	0.59
−11 ppm (PP)	–	0.089	0.144	0.039	0.025
K. pneumoniae:					
Resonance	T_1 in DOPC [s]			T_1 in PC/SM/Cholesterol [s]	
	25 °C			25 °C	15 °C
−1 ppm (P)	0.897			0.847	0.74
−10 ppm (PP)	0.424			1.5	1.023
−13 ppm (PP)	0.448			1.069	0.856
+20 ppm (Pn)	2.961			1.4	0.967
E. coli:					
Resonance	T_1 in DOPC [s]			T_1 in PC/SM/Chol [s]	
	25 °C			25 °C	15 °C
−1 ppm (P)	0.904			0.976	0.849
−7 ppm (PP)	0.846			0.375	0.422
−11 ppm (PP)	0.882			0.301	0.127

Preferential partitioning of LPS into the laterally separated ternary lipid membrane is consistent with the observed ordering effect of LPS on cholesterol and SM, seen in the ^{13}C MAS NMR data. This was investigated directly by following nuclear relaxation in ^{31}P reporters, intrinsic to LPS pyrophosphates in all species, as well as of phosphonates in LPS from *K. pneumoniae*. LPS from *B. melitensis*, a pathogen capable of invading macrophages in a raft-mediated fashion, was observed to lose motional freedom in the ternary lipid membrane, which is consistent with partitioning into the ordered cholesterol-rich domains. Interestingly, *in vivo*, intraperitoneal infection of mice with attenuated *B. abortus* leads to the formation of intracellular vesicles enriched in LPS, which are then recycled to the cell surface in association with MHC class II (MHC-II) where they form macrodomains. In this fashion, *B. abortus* LPS significantly impairs the presentation of peptides to specific CD4+ T cell hybridomas (reviewed in [55]) Thus, the results reported here are consistent with those observations and may provide a biophysical explanation for the observations *in vivo*.

Pyrophosphate relaxation from *K. pneumoniae* LPS revealed somewhat unusual motional behaviour, which is consistent with pyrophosphorylation sites located within lipid A where relaxation is dominated by membrane thermal undulations, readily suppressed by cholesterol. Relaxation from klebsiellar LPS phosphonates conclusively points to reduced mobility within the ternary lipid mixture and preferential partitioning of LPS into ordered domains. Pyrophosphate relaxation from *E. coli* LPS also revealed a marked reduction in molecular mobility within the ternary mixtures, indicative of LPS preference for the ordered lateral environment. LPS phosphorus mobility was observed to occur on the slow time scale in the ternary system, despite slight variation in the ^{31}P dynamics within pyrophosphate groups.

The fine detail on molecular and segmental mobility, obtained from ^{31}P relaxation measurements, emphasises the advantage of using ^{31}P MAS NMR in studies of mixed lipid membranes. Such information is essential in untangling non-cooperative modes of segmental dynamics from cooperative molecular and membrane mobility, which remain hidden in ^{1}H relaxation studies due to the strong proton couplings within atomic chains.

This study suggests that LPS, bound to lipid membranes, is segregated with preference into ordered cholesterol/SM-rich lateral domains, raft analogues. It is recognised that during LPS-mediated activation of TLR-4 the receptor is transiently localised within the

ordered lipid domains [50]. The TLR-4-mediated response to bacterial LPS depends on the interaction of soluble LPS with LBP or of membrane-associated LPS with CD14, a GPI-anchored protein normally resident within the lipid raft environment. We hypothesise that the observed preference of LPS to segregate into the ordered cholesterol/SM-rich domains has been a contributing factor in the evolutionary drive within eukaryotic cells to develop a GPI-anchored sensory response element, CD-14, which resides within cholesterol/SM-rich lipid rafts as the first line of bacterial detection.

5. Conclusions

Interactions between LPS and model membranes with raft-like properties were studied using solid state ^{13}C and ^{31}P MAS NMR spectroscopy. The presence of LPS in ternary PC/SM/cholesterol membranes was found to have an overall ordering effect on the membrane lipid. All LPS species were pyrophosphorylated and klebsiellar LPS was phosphonylated, as well. Phosphorus-31 longitudinal relaxation was used to follow changes in the LPS mobility on incorporation into the ternary lipid mixture and a reduction in T_1 was interpreted as indicative of preferential partitioning of LPS into ordered lipid phases.

Acknowledgements

References

[1] S. Akira, Mammalian Toll-like receptors, Curr. Opin. Immunol. 15 (2003) 5–11.
[2] A. Martirosyan, E. Moreno, J.P. Gorvel, An evolutionary strategy for a stealthy intracellular Brucella pathogen, Immunol. Rev. 240 (2011) 211–234.
[3] E. Barquero-Calvo, R. Conde-Alvarez, C. Chacon-Diaz, L. Quesada-Lobo, A. Martirosyan, C. Guzman-Verri, M. Iriarte, M. Mancek-Keber, R. Jerala, J.P. Gorvel, I. Moriyon, E. Moreno, E. Chaves-Olarte, The differential interaction of Brucella and Ochrobactrum with innate immunity reveals traits related to the evolution of stealthy pathogens, PLoS One 4 (2009).
[4] C.R.H. Raetz, C. Whitfield, Lipopolysaccharide endotoxins, Annu. Rev. Biochem. 71 (2002) 635–700.
[5] L.J. Pike, Lipid rafts: bringing order to chaos, J. Lipid Res. 44 (2003) 655–667.
[6] K. Simons, E. Ikonen, Functional rafts in cell membranes, Nature 387 (1997) 569–572.
[7] J.D. Correia, K. Soldau, U. Christen, P.S. Tobias, R.J. Ulevitch, Lipopolysaccharide is in close proximity to each of the proteins in its membrane receptor complex — transfer from CD14 to TLR4 and MD-2, J. Biol. Chem. 276 (2001) 21129–21135.
[8] D.A. Brown, J.K. Rose, Sorting of GPI-anchored proteins to glycolipid-enriched membrane subdomains during transport to the apical cell-surface, Cell 68 (1992) 533–544.
[9] G. Schmitz, E. Orso, CD14 signalling in lipid rafts: new ligands and co-receptors, Curr. Opin. Lipidol. 13 (2002) 513–521.
[10] J. Cuschieri, J. Billgren, R.V. Maier, Phosphatidylcholine-specific phospholipase C (PC-PLC) is required for LPS-mediated macrophage activation through CD14, J. Leukoc. Biol. 80 (2006) 407–414.
[11] M.B. Fessler, J.S. Parks, Intracellular lipid flux and membrane microdomains as organizing principles in inflammatory cell signaling, J. Immunol. 187 (2011) 1529–1535.
[12] F.S. Vieira, G. Correa, M. Einicker-Lamas, R. Coutinho-Silva, Host-cell lipid rafts: a safe door for micro-organisms? Biol. Cell 102 (2010) 391–407.
[13] A. Hartlova, L. Cerveny, M. Hubalek, Z. Krocova, J. Stulik, Membrane rafts: a potential gateway for bacterial entry into host cells, Microbiol. Immunol. 54 (2010) 237–245.
[14] S. Olsson, R. Sundler, The role of lipid rafts in LPS-induced signaling in a macrophage cell line, Mol. Immunol. 43 (2006) 607–612.
[15] A. Naroeni, F. Porte, Role of cholesterol and the ganglioside GM(1) in entry and short-term survival of Brucella suis in murine macrophages, Infect. Immun. 70 (2002) 1640–1644.
[16] S. Kim, M. Watarai, H. Suzuki, S. Makino, T. Kodama, T. Shirahata, Lipid raft microdomains mediate class A scavenger receptor-dependent infection of Brucella abortus, Microb. Pathog. 37 (2004) 11–19.
[17] F. Ciesielski, B. Davis, M. Rittig, B.B. Bonev, P. O'Shea, Receptor-independent interaction of bacterial lipopolysaccharide with lipid and lymphocyte membranes; the role of cholesterol, PLoS One 7 (2012) e38677.
[18] J. Kubiak, J. Brewer, S. Hansen, L.A. Bagatolli, Lipid lateral organization on giant unilamellar vesicles containing lipopolysaccharides, Biophys. J. 100 (2011) 978–986.
[19] C. Forestier, E. Moreno, S. Meresse, A. Phalipon, D. Olive, P. Sansonetti, J.P. Gorvel, Interaction of Brucella abortus lipopolysaccharide with major histocompatibility complex class II molecules in B lymphocytes, Infect. Immun. 67 (1999) 4048–4054.
[20] C. Forestier, F. Deleuil, N. Lapaque, E. Moreno, J.P. Gorvel, Brucella abortus lipopolysaccharide in murine peritoneal macrophages acts as a down-regulator of T cell activation, J. Immunol. 165 (2000) 5202–5210.
[21] R.F.M. de Almeida, A. Fedorov, M. Prieto, Sphingomyelin/phosphatidylcholine/cholesterol phase diagram: boundaries and composition of lipid rafts, Biophys. J. 85 (2003) 2406–2416.
[22] J. Velasco, J.A. Bengoechea, K. Brandenburg, B. Lindner, U. Seydel, D. Gonzalez, U. Zahringer, E. Moreno, I. Moriyon, Brucella abortus and its closest phylogenetic relative, Ochrobactrum spp., differ in outer membrane permeability and cationic peptide resistance, Infect. Immun. 68 (2000) 3210–3218.
[23] R.W. Martin, K.W. Zilm, Variable temperature system using vortex tube cooling and fiber optic temperature measurement for low temperature magic angle spinning NMR, J. Magn. Reson. 168 (2004) 202–209.
[24] F. Ciesielski, D.C. Griffin, M. Rittig, B.B. Bonev, High-resolution J-coupled C-13 MAS NMR spectroscopy of lipid membranes, Chem. Phys. Lipids 161 (2009) 77–85.
[25] S.R. Hartmann, E.L. Hahn, Nuclear double resonance in rotating frame, Phys. Rev. 128 (1962) 2042–2053.
[26] G. Metz, X.L. Wu, S.O. Smith, Ramped-amplitude cross-polarization in magic-angle-spinning NMR, J. Magn. Reson., Ser. A 110 (1994) 219–227.
[27] B.M. Fung, A.K. Khitrin, K. Ermolaev, An improved broadband decoupling sequence for liquid crystals and solids, J. Magn. Reson. 142 (2000) 97–101.
[28] V. Zorin, F. Ciesielski, D.C. Griffin, M. Rittig, B.B. Bonev, Heteronuclear chemical shift correlation and J-resolved MAS NMR spectroscopy of lipid membranes, Magn. Reson. Chem. 48 (2010) 925–934.
[29] J. Forbes, C. Husted, E. Oldfield, High-field, high-resolution proton magic-angle sample-spinning nuclear magnetic-resonance spectroscopic studies of gel and liquid-crystalline lipid bilayers and the effects of cholesterol, J. Am. Chem. Soc. 110 (1988) 1059–1065.
[30] O.A. Valueva, D. Rakhuba, A.S. Shashkov, E.L. Zdorovenko, E. Kiseleva, G. Novik, Y.A. Knirel, Structure of the major O-specific polysaccharide from the lipopolysaccharide of Pseudomonas fluorescens BIM B-582: identification of 4-Deoxy-D-xylo-hexose as a component of bacterial polysaccharides, J. Nat. Prod. 74 (2011) 2161–2167.
[31] K. Nomura, M. Maeda, K. Sugase, S. Kusumoto, Lipopolysaccharide induces raft domain expansion in membrane composed of a phospholipid–cholesterol–sphingomyelin ternary system, Innate Immun. 17 (2011) 256–268.
[32] R. Conde-Alvarez, V. Arce-Gorvel, M. Iriarte, M. Mancek-Keber, E. Barquero-Calvo, L. Palacios-Chaves, C. Chacon-Diaz, E. Chaves-Olarte, A. Martirosyan, K. von Bargen, M.J. Grillo, R. Jerala, K. Brandenburg, J.A. Bengoechea, E. Llobet, E. Moreno, I. Moriyon, J.P. Gorvel, The lipopolysaccharide core of Brucella abortus acts as a shield against innate immunity recognition, PLoS Pathog. 8 (2012).
[33] N. Sanghera, B.E.F.S. Correia, J.R.S. Correia, C. Ludwig, S. Agarwal, H.K. Nakamura, K. Kuwata, E. Samain, A.C. Gill, B.B. Bonev, T.J.T. Pinheiro, Deciphering the molecular details for the binding of the prion protein to main ganglioside GM1 of neuronal membranes, Chem. Biol. 18 (2011) 1422–1431.
[34] J. Forbes, J. Bowers, X. Shan, L. Moran, E. Oldfield, M.A. Moscarello, Some new developments in solid-state nuclear magnetic-resonance spectroscopic studies of lipids and biological-membranes, including the effects of cholesterol in model and natural systems, J. Chem. Soc., Faraday Trans. 1 84 (1988) 3821–3849.
[35] G.P. Holland, T.M. Alam, Multi-dimensional H-1-C-13 HETCOR and FSLG-HETCOR NMR study of sphingomyelin bilayers containing cholesterol in the gel and liquid crystalline states, J. Magn. Reson. 181 (2006) 316–326.
[36] J. Velasco, C. Romero, I. Lopez-Goni, J. Leiva, R. Diaz, I. Moriyon, Evaluation of the relatedness of Brucella spp. and Ochrobactrum anthropi and description of Ochrobactrum intermedium sp. nov., a new species with a closer relationship to Brucella spp, Int. J. Syst. Bacteriol. 48 (1998) 759–768.
[37] B. Bonev, A. Watts, M. Bokvist, G. Grobner, Electrostatic peptide–lipid interactions of amyloid-beta peptide and pentalysine with membrane surfaces monitored by P-31 MAS NMR, Phys. Chem. Chem. Phys. 3 (2001) 2904–2910.
[38] B.B. Bonev, Y.H. Lam, G. Anderluh, A. Watts, R.S. Norton, F. Separovic, Effects of the eukaryotic pore-forming cytolysin equinatoxin II on lipid membranes and the role of sphingomyelin, Biophys. J. 84 (2003) 2382–2392.
[39] X.Y. Wang, A.A. Ribeiro, Z.Q. Guan, C.R.H. Raetz, Identification of undecaprenyl phosphate-beta-D-galactosalmine in Francisella novicida and its function in lipid A modification, Biochemistry 48 (2009) 1162–1172.
[40] B.B. Bonev, E. Breukink, E. Swiezewska, B. De Kruijff, A. Watts, Targeting extracellular pyrophosphates underpins the high selectivity of nisin, FASEB J. 18 (2004) 1862–1869.
[41] J. Vestergren, A.G. Vincent, M. Jansson, P. Persson, U. Ilstedt, G. Grobner, R. Giesler, J. Schleucher, High-resolution characterization of organic phosphorus in soil extracts using 2D (1)H–(31)P NMR correlation spectroscopy, Environ. Sci. Technol. 46 (2012) 3950–3956.
[42] M.I. Torres-Sanchez, C. Zaccaria, B. Buzzi, G. Miglio, G. Lombardi, L. Polito, G. Russo, L. Lay, Synthesis and biological evaluation of phosphono analogues of capsular polysaccharide fragments from Neisseria meningitidis A, Chem. Eur. J. 13 (2007) 6623–6635.

[43] J.H. Davis, The description of membrane lipid conformation, order and dynamics by H-2-NMR, Biochim. Biophys. Acta 737 (1983) 117–171.

[44] P. Garidel, J. Howe, K. Brandenburg, Thermodynamic analysis of the interaction of lipopolysaccharides with cationic compounds, Eng. Life Sci. 8 (2008) 523–529.

[45] M.W. Hornef, M.J. Wick, M. Rhen, S. Normark, Bacterial strategies for overcoming host innate and adaptive immune responses, Nat. Immunol. 3 (2002) 1033–1040.

[46] S. Manes, G. del Real, C. Martinez-A, Pathogens: raft hijackers, Nat. Rev. Immunol. 3 (2003) 557–568.

[47] M. Triantafilou, K. Miyake, D.T. Golenbock, K. Triantafilou, Mediators of innate immune recognition of bacteria concentrate in lipid rafts and facilitate lipopolysaccharide-induced cell activation, J. Cell Sci. 115 (2002) 2603–2611.

[48] M.J. Duncan, G.J. Li, J.S. Shin, J.L. Carson, S.N. Abraham, Bacterial penetration of bladder epithelium through lipid rafts, J. Biol. Chem. 279 (2004) 18944–18951.

[49] C.F. Fortin, O. Lesur, T. Fulop, Effects of TREM-1 activation in human neutrophils: activation of signaling pathways, recruitment into lipid rafts and association with TLR4, Int. Immunol. 19 (2007) 41–50.

[50] M. Triantafilou, S. Morath, A. Mackie, T. Hartung, K. Triantafilou, Lateral diffusion of Toll-like receptors reveals that they are transiently confined within lipid rafts on the plasma membrane, J. Cell Sci. 117 (2004) 4007–4014.

[51] X.W. Zhu, J.S. Owen, M.D. Wilson, H.T. Li, G.L. Griffiths, M.J. Thomas, E.M. Hiltbold, M.B. Fessler, J.S. Parks, Macrophage ABCA1 reduces MyD88-dependent Toll-like receptor trafficking to lipid rafts by reduction of lipid raft cholesterol, J. Lipid Res. 51 (2010) 3196–3206.

[52] N. Sanghera, Bruno E.F.S. Correia, Joana R.S. Correia, C. Ludwig, S. Agarwal, Hironori K. Nakamura, K. Kuwata, E. Samain, Andrew C. Gill, Boyan B. Bonev, Teresa J.T. Pinheiro, Deciphering the molecular details for the binding of the prion protein to main ganglioside GM1 of neuronal membranes, Chem. Biol. 18 (2011) 1422–1431.

[53] Z.M. Zhou, A.A. Ribeiro, C.R.H. Raetz, High-resolution NMR spectroscopy of lipid A molecules containing 4-amino-4-deoxy-L-arabinose and phosphoethanolamine substituents — different attachment sites on lipid A molecules from NH4VO3-treated *Escherichia coli* versus kdsA mutants of *Salmonella typhimurium*, J. Biol. Chem. 275 (2000) 13542–13551.

[54] Z.M. Zhou, A.A. Ribeiro, S.H. Lin, R.J. Cotter, S.I. Miller, C.R.H. Raetz, Lipid A modifications in polymyxin-resistant *Salmonella typhimurium* — PMRA-dependent 4-amino-4-deoxy-L-arabinose, and phosphoethanolamine incorporation, J. Biol. Chem. 276 (2001) 43111–43121.

[55] N. Lapaque, F. Forquet, C. de Chastellier, Z. Mishal, G. Jolly, E. Moreno, I. Moriyon, J.E. Heuser, H.T. He, J.P. Gorvel, Characterization of *Brucella abortus* lipopolysaccharide macrodomains as mega rafts, Cell. Microbiol. 8 (2006) 197–206.

[56] J. Kubler-Kielb, E. Vinogradov, The study of the core part and non-repeating elements of the O-antigen of Brucella lipopolysaccharide, Carbohydr. Res. 366 (2013) 33–37.